Sensorless direct torque control of three-phase induction motor using sliding mode control strategy

Marcos Vinicius Lazarini and Ernesto Ruppert Filho
School of Electrical and Computer Engineering
Campinas State University – Brazil
lazarini@dsce.fee.unicamp.br, ruppert@fee.unicamp.br

***Abstract*—A variable speed drive system using three-phase induction motor is presented. The system comprises a direct torque control strategy using sliding mode control and space vector modulation method. The sensorless strategy was based on a high efficiency model-reference adaptative system that is able to operate in a wide speed range. This method was designed to combine the good characteristics of the direct torque and the sliding mode controllers, and operate with constant switching frequency provided by the space vector modulation method. Simulation and experimental results are presented showing the behavior of the proposed method.**

***Keywords*— induction motor, sensorless, sliding mode, torque control**

I. Introduction

Three-phase induction machines have a main role in today's industrial applications. Due to its ruggedness and very low maintenance requirements, they turned out to be widely used today. With the emerging of advanced control techniques starting in the late 80's, the induction machine became even more interesting, for variable speed drive systems.

Among many control methods of induction machines, one of the most important today is the Direct Torque Control (*DTC*) method, introduced in [1] and [2]. It can provide a very fast, accurate and reliable flux control and torque response, achieving a high degree of accuracy and being somewhat simpler than the previous methods, like the field oriented control. Instead of using the classical approach with switching logic relays and a switching vector table operating in variable switching frequency, higher accuracy can be achieved using a fixed switching frequency space vector modulation (SVM) [3]. Different strategies considering various aspects are shown in [4]. In this paper, it is implemented the SVM strategy applied to the DTC algorithm.

Sliding Mode Control theory plays a main role in variable structure control research. As a discontinuous control method, it introduces discontinuities in the mathematical model. Until recently, solving these equations was a difficult task, but new mathematical tools and theorems emerged and now sliding mode control is gaining much more attention. A typical discontinuous function is the sign function but in order to achieve good performance in discrete-time systems, it is usually replaced by a linear function, to obtain closer behavior. As a discontinuous control, the sliding mode control has key advantages like the ability to be a very robust control, in many cases invariant to uncertainty and disturbances [5]; it has also properties of order reduction, decoupling design procedure and simple implementation in electric drives, since they have a natural "on-off" operating mode [6]. When designed following the DTC control rules (controlling the stator flux and electromagnetic torque) it behaves much like a DTC controller and produces good results [3].

Sensorless drives are becoming more and more important as they can eliminate the shaft speed sensor and also the complex and costly flux and torque sensors, still with good and accurate response. Monitoring only the stator current and stator voltages, it is possible to estimate the necessary control variables. The estimator type used here, a model-reference adaptative system (*MRAS*) [7], achieved a good accuracy, although the low speed estimation is still an unsolved problem. The observer presented in [8] is an improved model, and it is implemented in this paper.

II. Direct Torque Control

From the induction machine mathematical model, the main equation of the direct torque control method [9] defines a relationship between the electromagnetic torque and the angle between the stator and rotor fluxes shown in (1)

$$T_{em} = \frac{3}{2}\frac{P}{2}\frac{L_m}{L_{lr}L_{ls}}|\psi_s||\psi_r|\sin(\delta) \tag{1}$$

where T_{em} is the electromagnetic torque, P is the number of poles, ψ_s and ψ_r are, in order, the stator and rotor linkage fluxes, L_{ls} and L_{lr} are the stator and rotor leakage inductances, and δ is the angle between the stator flux and rotor flux vectors. Ignoring parameter variations, as long as the stator flux magnitude remains constant, the rotor flux magnitude will be constant too and, from (1), the electromagnetic torque is related only to the flux angle difference δ.

The stator flux linkage vector depends directly on the stator voltages [10] and can be calculated as

$$\underline{\psi_s} = \int (\underline{V_s} - r_s\underline{i_s})dt \tag{2}$$

where V_s is the terminals voltage of the machine, r_s is the stator resistance, and i_s is the stator current. The underline denotes a 2-coordinate vector variable, the stationary dq coordinate system, which is assumed along this work, unless when noted otherwise. In most cases the ohmic drop is small and can be neglected, and the flux variations can be approximated

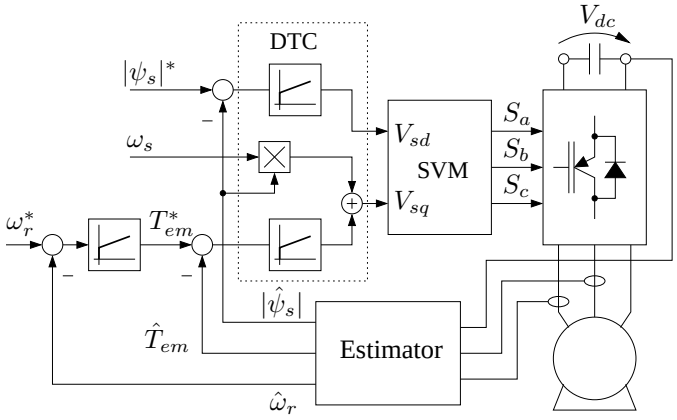

Fig. 1. Speed controler and DTC block diagram

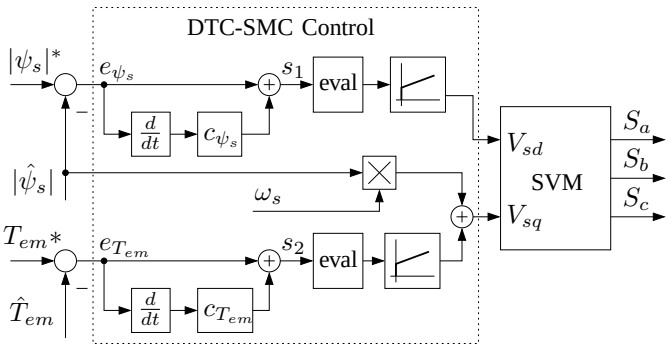

Fig. 2. DTC-Sliding mode control law

considering $r_s = 0$. Equation (2) shows that the flux variation is then due only to the applied stator voltage. In other words, to control the stator winding linkage flux vector, the inverter generates a stator voltage vector that moves the stator flux to a convenient position; this stator voltage vector is recalculated at each switching period.

The control algorithm calculates the magnitude and the angle to move the stator flux winding linkage vector to a position producing torque according to (1). Flux vector magnitude is usually hold at rated value to generate the fastest possible response, but it is also possible to work with an underrated flux vector magnitude, in order to have lower acoustic noise and a better energy efficiency machine in specific situations at the cost of a slower response [1].

In the classical DTC control, the traditional two-level inverter can only produce 6 active and 2 inactive voltage vectors. This is an important constrain to the system and it is the cause of torque ripple in steady-state situations. Instead of the classical approach [1], using the space vector modulation strategy for a given fixed-time switching period, it is possible to generate a much wider range of average voltage vectors, producing a much more smooth and accurate response.

In order to find the correct magnitude and the new stator winding linkage flux vector position, the induction machine stator voltage equations [11] can be re-written. From [4], the dq components in the stationary reference frame are

$$V_{sd} = r_s \cdot i_{sd} + \frac{d\psi_s^*}{dt} \approx \frac{d\psi_s^*}{dt} \quad (3)$$

$$V_{sq} = r_s \cdot i_{sq} + \omega_s \cdot \psi_s^* = \omega_s \cdot \psi_s^* + \frac{r_s}{\psi_s^*} T_{em} \quad (4)$$

where superscripts * means reference value and ω_s is the synchonous angular speed of the stator flux vector. The above equations show, for a constant magnitude stator flux vector, that the d component of the stator voltage only affects the stator flux and can be used to control it directly. The q component of the stator voltage affects the torque variable, and if the term $\omega_s \psi_s^*$ is decoupled, it can be used to control the produced torque.

Fig. 1 illustrates the control block diagram of system. The selected box encloses the control block of this DTC scheme; the implemented algorithm is quite represented in Fig. 2 and is discussed in details in the next section. Of the two PI controllers shown, although recommended by some authors [3], one controller can be removed without significant penalty to the dynamics of the system. Because V_{sd} can be approximated to the variation of the stator flux according to (3), the stator winding linkage flux output error ($|\psi_s|^* - |\hat{\psi}_s|$) already gives the proper variation and can drive V_{sd} directly.

III. Sliding Mode Control

Sliding Mode Control (*SMC*) is presented today as a feasible alternative to implement a robust control, taking advantage of the "on-off" inverter switches characteristics and its inherent discontinuous algorithm to control the electrical machine. However this causes a major disvantage: a variable switching frequency. To get a fixed switching frequency operation it is used the space vector modulation strategy, while preserving the good characteristics of the SMC. Implementation in discrete-time digital signal processor also demands changes to avoid unwanted chattering, as explained below.

The sliding mode controller was designed to operate over the same variables used in the DTC method. The main goal of this approach is to obtain a sliding mode controller with all the qualities of DTC, which calculates the optimal stator voltage vector to maintain the stator winding linkage flux magnitude and angle within the desired ranges to produce the desired electromagnetic torque, and outputs this reference to the SVM inverter. The implemented control block diagram is shown within a dotted rectangle in Fig. 2.

In this figure, the *eval* block usually is any function of the following: sign, relay or linear with saturation, as shown in Fig. 3. Both the sign and the relay functions alone do not perform accurately in a discrete-time system, resulting in

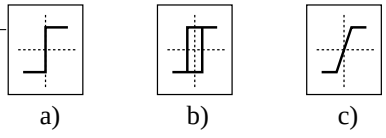

Fig. 3. Typical *eval* functions: a) sign, b) relay, c) linear with saturation

oscillations and undesired chattering. Using a linear function with a proper slope gain and saturation levels provides much better results in reducing oscillations while still maintaining the properties of sliding mode [6].

The individual sliding surfaces are designed to behave in a similar way to the DTC control. First it is defined the error functions between the reference and the estimated values

$$\begin{aligned} e_{\psi_s} &= |\psi_s|^* - |\hat{\psi}_s| \\ e_{T_{em}} &= T^*_{em} - \hat{T}_{em} \end{aligned} \tag{5}$$

where the hat symbol means estimated quantity and e is an error value to be minimized.

The *sliding surface* set S is defined from (5)

$$S = \begin{bmatrix} s_1 \\ s_2 \end{bmatrix} = \begin{bmatrix} e_{\psi s} & + & c_{\psi_s} \cdot \dfrac{d}{dt}\left(e_{\psi_s}\right) \\ e_{T_{em}} & + & c_{T_{em}} \cdot \dfrac{d}{dt}\left(e_{T_{em}}\right) \end{bmatrix} \tag{6}$$

where $c_{\psi s}$ e $c_{T_{em}}$ are constants to be defined according to the desired dynamics response.

The surfaces s_1 and s_2 were defined according to (3) and (4), using the same idea that the d stator voltage component is related with stator flux and q stator voltage component is related with electromagnetic torque.

Therefore, the control law is proposed in a similar way

$$\begin{aligned} V_{sd} &= \left(KP_\psi + KI_\psi \frac{1}{s}\right) \text{eval}(s_1) \\ V_{sq} &= \left(KP_T + KI_T \frac{1}{s}\right) \text{eval}(s_2) + \omega_s \hat{\psi}_s \end{aligned} \tag{7}$$

where KP_ψ, KI_ψ, KP_T and KI_T are PI gains. The *eval* function is implemented as a linear gain with saturation

$$\text{eval}(x) = \begin{cases} xk_{ev} & \text{if lower limit} < x < \text{upper limit}, \\ \text{upper limit} & \text{if } x \geq \text{upper limit}, \\ \text{lower limit} & \text{if } x \leq \text{lower limit}. \end{cases} \tag{8}$$

where k_{ev} is a constant related to the system dynamics.

The system's state can start outside the sliding surface but it will be driven toward the sliding surface as control effort will be produced according to (7) to reduce the errors (5) and reach $S = 0$. This is the *reaching phase*.

When the system state reaches the $S = 0$ surface and enters in the *sliding phase* or sliding mode, the same control law (7) restricts the state to the slide surface S and the system actions is governed by the dynamics imposed by $S = 0$ only. The system state is not allowed to leave the S surface, generating a quick and large enough control effort to keep the system state very close to the sliding surface. This intense reaction, besides producing a very fast response, can also generating undesired ripple in discrete-time systems, as a side-effect of limit cycle in the state space plane. Close to the steady state, using the linear function from Fig. 3 instead of sign function, the system response is fast and stable.

The equivalent control is a fundamental theory in variable structure systems that simplify the discontinuous system analysis, replacing discontinuous equations with continuous equivalents, where its trajectory is the sliding surface itself. Therefore it is possible to calculate traditional coefficients, like damping factor and natural frequency for a step response for example. A more detailed view of the background theory and sliding surface design can be seen in [6].

IV. Estimator Subsystem

The adopted estimation structure is a model-reference adaptative system (*MRAS*) [7], and it consists of three stage system: two independent estimators and an adaptive mechanism to correct the estimations, producing the final result. An improved model, discussed in [8], was the basic scheme. The adopted structure is presented in Fig. 4.

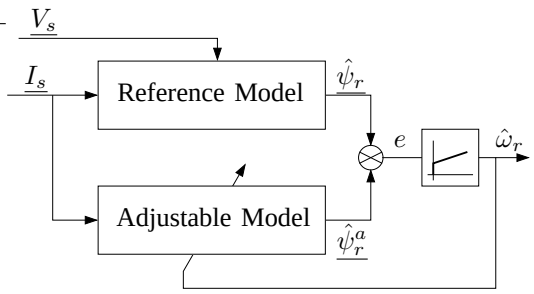

Fig. 4. MRAS block diagram

In the following subsections, the various parts of the estimator are discussed. The two independent estimators produce a rotor flux estimation, and the final rotor speed is then calculated from these values.

A. Reference Model

The reference model discussed here is adaptive itself. The rotor winding linkage flux is calculated from a closed loop system presented in Fig. 5. This method, analyzed in details in [8], uses two distinct reference frames to get an improved estimation. Two reference frames were used during calculations: the rotor flux reference frame (named dq) and the stationary reference frame (named $\alpha\beta$), as presented in the figure.

Using the rotor flux reference frame, the rotor flux equations are simpler to be described: the d axis is aligned with the rotor flux and receives all the flux contribution, while the q is perpendicular to the rotor flux, receiving no contribution. Thus, the rotor flux in rotor flux reference frame can be written as

$$\underline{\psi_r^{r\prime}} = \begin{bmatrix} \psi^r_{rd} \\ \psi^r_{rq} \end{bmatrix} = \begin{bmatrix} \frac{L_m}{1+sT_r} i^r_{sd} \\ 0 \end{bmatrix} \tag{9}$$

where L_m is the machine magnetizing self-inductance, T_r is the rotor time-constant and superscript r denotates variable in the rotor flux reference frame.

Performing a coordinate system conversion of (9) back to the stationary reference frame, the stator flux can be calculated from the rotor flux and stator current as

$$\underline{\hat{\psi}^i_s} = \frac{L_m}{L_{lr}} \underline{\psi'_r} + \frac{L_{ls}L_{lr} - L_m^2}{L_{lr}} \underline{i_s}. \tag{10}$$

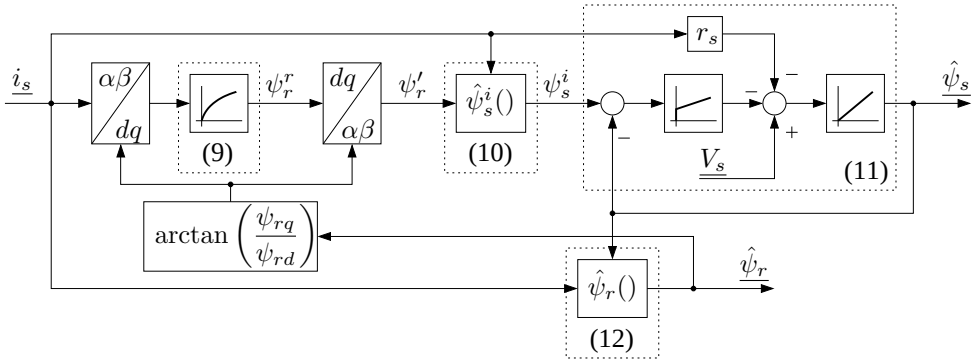

Fig. 5. MRAS Reference Model

The superscript i denotates the stator flux calculated from the stator currents.

The reference model also calculates the stator flux using another method, through a feedback system where the stator flux $\hat{\psi}_s$ is the feedback variable. A PI compensator – represented by $(KP_\psi^e + \frac{KI_\psi^e}{s})$ – dictates the error contribution between the two flux estimations (10) and (11)

$$\underline{\hat{\psi}_s} = \frac{1}{s}\left(\underline{V_s} - r_s\underline{i_s} - \left(KP_\psi^e + \frac{KI_\psi^e}{s}(\underline{\hat{\psi}_s} - \underline{\hat{\psi}_s^i})\right)\right). \quad (11)$$

The superscript e is used to avoid confusion with others PI compensators gains. This model uses stator currents and voltages, and the PI compensator is used to correct pure integrator errors and small stator resistance variation through the voltage model estimation.

The reference model final rotor flux estimation value $\hat{\psi}_r$ is calculated from stator voltages and currents by

$$\underline{\hat{\psi}_r} = \frac{L_{lr}}{L_m}\underline{\hat{\psi}_s} - \frac{L_{ls}L_{lr} - L_m^2}{L_m}\underline{i_s}. \quad (12)$$

B. Adjustable Model

The adjustable or adaptive model equation is simpler and is obtained from the current model of the machine equations in stationary reference frame [7] using stator currents and rotor angular velocity

$$\underline{\hat{\psi}_r^a} = \begin{bmatrix} (-1/T_r) & -\hat{\omega}_r \\ \hat{\omega}_r & (-1/T_r) \end{bmatrix} \underline{\hat{\psi}_r^a} + \frac{L_m}{T_r}\underline{i_s} \quad (13)$$

The superscript a denotates the stator flux calculated from the adaptative model.

C. Rotor speed estimation

With the rotor flux estimation from two methods – the voltage model $\underline{\hat{\psi}_r}$ (reference model) and the current model $\underline{\hat{\psi}_r^a}$ (adaptive model) – the rotor speed $\hat{\omega}_r$ can be calculated with a PI adaptation mechanism by

$$\hat{\omega}_r = \left(KP_\omega + \frac{KI_\omega}{s}\right) \cdot e \quad (14)$$

where

$$e = \hat{\psi}_{rd}^a \cdot \hat{\psi}_{rq} - \hat{\psi}_{rq}^a \cdot \hat{\psi}_{rd} \quad (15)$$

is the cross-error between the adjustable and reference models.

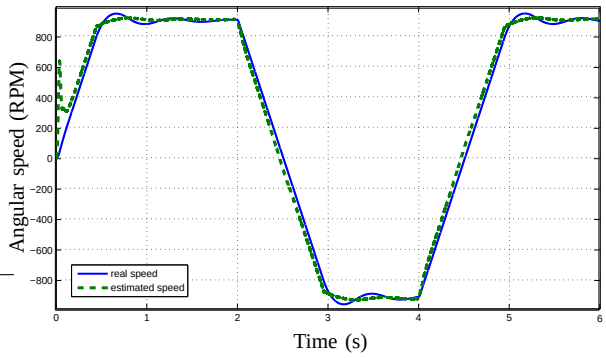

Fig. 6. System response to the reference speed step change ±0.5 pu

V. Simulation Results

The above proposed method was simulated using Matlab/Simulink. The complete system was implemented, in a closed-loop speed estimation feedback.

The machine parameters are: $P = 2.2$ kW, $V_s = 220$ V, $I_N = 9$ A, $f_s = 60$ Hz, $P = 2$ pole pairs, $r_s = 0.6853\ \Omega$, $r_r = 0.6688\ \Omega$, $L_{ls} = L_{lr} = 6.281$ mH, $L_m = 713,1$ mH. The machine calculated rated values are $T_{em} = 12$ Nm and $\psi_s = 0.48$ Wb. A switching frequency of 10 kHz was used.

The simulated scenario covers the following situations: a step change in the speed reference (from 0.5 pu to -0.5 pu) with no load attached, a step change in torque (from 0 to 0.5 pu) and a very low speed operation (30 rpm) with no load.

The results of step change in the speed reference are presented in Fig. 6, where the real speed ω_r and estimated speed $\hat{\omega}_r$ are shown. Although with some oscilation, the estimation tracked the real speed very close and it was able to follow the rotor speed within 5% accuracy most of the time.

The stator flux was also estimated and is shown in Fig. 7. During the startup phase, the stator flux grows from zero to the rated value. The flux magnitude is held constant from this moment on, and this can be verified as the stator flux locus in a xy plane is a circle.

The step change in the torque, from 0 to 0.5 pu at 50% rated speed is shown in Fig. 8. Operating at no load, the speed estimation almost matches the real speed; with 0.5 pu load, the system settle to a new steady state, where the difference

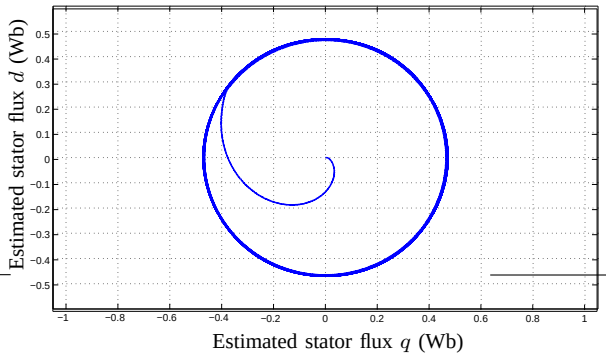

Fig. 7. Stator flux during the speed step experiment

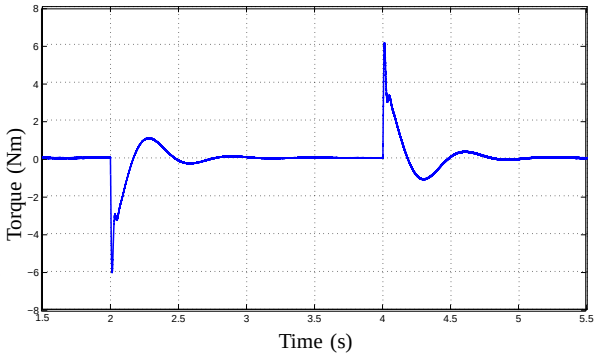

Fig. 10. Torque response at low speed change between 1 Hz and 2 Hz

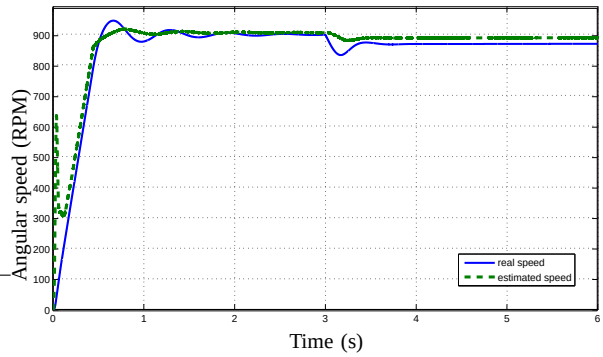

Fig. 8. System response to the load torque step change 0.5 pu

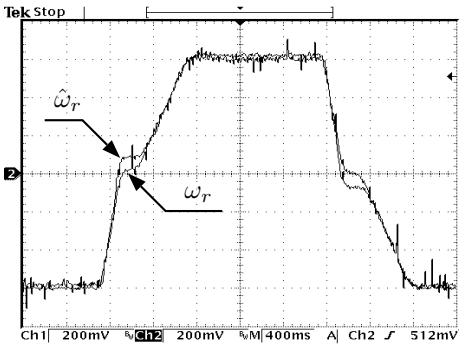

Fig. 11. Real and estimaded rotor speed in step change, ±30 Hz (10 Hz/div)

between the real and the estimated speed is less than 2%.

Operating with no load at low speed (Fig. 9), the low stator voltages and low stator currents have an negative effect in the quality of the speed estimation. The estimator cannot compensate accordingly such problems and, operating at frequencies of about 1 Hz, the error between real and estimated speed grows to about 25%. Due to the poor estimation at this speed, the system take longer to reach a steady state. The torque responde is still fast, but generetes oscilation, as shown in Fig. 10.

VI. Experimental Results

The experimental setup consists of a DSP (Texas Instruments TMS320F2812) connected to an induction motor, driven by a 6 kW Semikron three-phase inverter (SKS 27F B6U + B6CI 10V06). No other microcontroler was used; the DSP performed all the necessary steps, timing and calculations. The switching frequency was defined as 10 kHz, and the dead-time was defined as 0.8 μs.

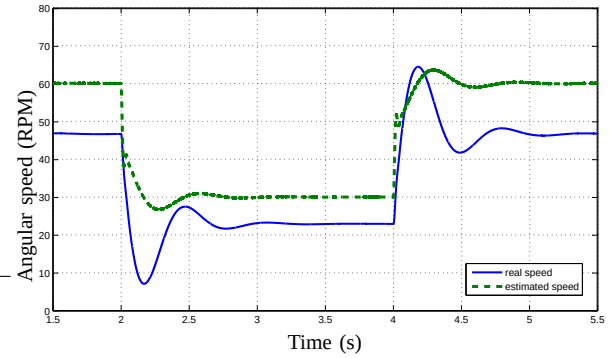

Fig. 9. Speed response at low speed change between 1 Hz and 2 Hz

The voltages and currents sampling frequency was defined as eight times the switching frequency (80 kHz) and a moving average filter with a uniform weight of $1/8$ was used to smooth the sampled signal. The machine parameters are the same from the simulation.

In the experiments, the following parameters were used in the controllers: $KP_\omega = 5$, $KI_\omega = 12000$; $KP^e_\psi = 40$, $KI^e_\psi = 5$ for both d and q axis; $KP_\psi = 2.2$, $KI_\psi = 04$; $KP_T = 10$, $KI_T = 100$; and for the outter speed loop, $KP = 1.6$, $KI = 0.05$.

Fig. 11 shows the speed reversal test, varying between +30 Hz and -30 Hz each 2s. In this test, the estimator gave good results, as both signals were almost superimposed; the steady state error is below 2%. The figure shows that the breaking phase is faster than the acceleration phase, because the friction force wasn't considered in the equations, but it wasn't negligible in this machine. Fig. 12 shows the developed torque for the same situation. It fluctuates around zero speed, as the estimator performance is worse at this region, but remain constant close to the allowed maximum (the rated value, 12 Nm). The estimated stator flux is also presented in Fig. 13, where its magnitude remains almost constant during the test.

In a much similar situation to the one presented in Fig.

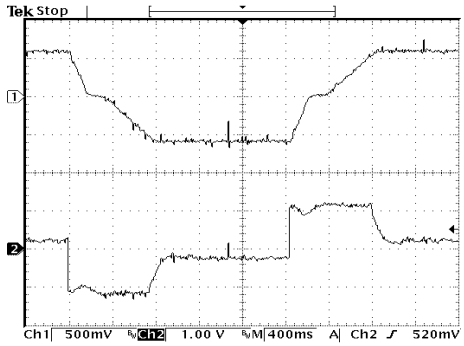

Fig. 12. Real speed and torque response in speed step change, ±30 Hz (25 Hz/div, 10 Nm/div)

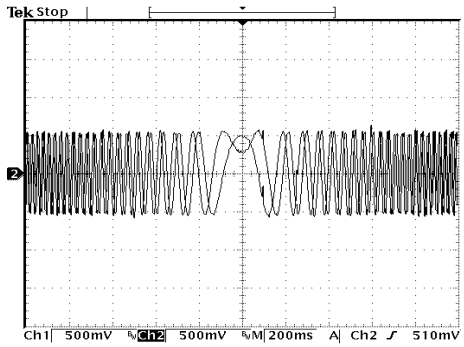

Fig. 13. Stator flux dq components, ±30 Hz (0.5 Wb/div)

8, the experimental setup produced the output in Fig. 14. Although the estimator was not capable of tracking the real speed closely, the oscillations were minimal.

A low speed operation of the experiments (Fig. 15) confirmed the expectations from the simulations, giving very similar results for the same conditions.

VII. Conclusion

During the simulations and experiments, the currently presented speed drive method performed well under a variety of the proposed conditions and the experiments validated the simulations. The association of the DTC control strategy with the space-vector modulation increased the accuracy of the results when compared to the classical DTC with relays

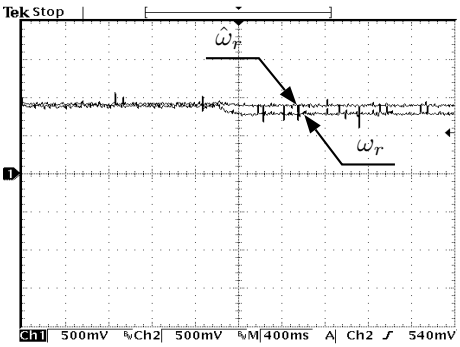

Fig. 14. Speed response to a 0.5 pu torque step change at 30 Hz

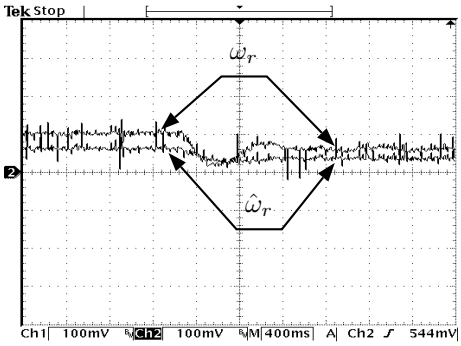

Fig. 15. Speed estimation at low speed, 2 Hz to 1 Hz (3.2 Hz/div)

switching logic, using a fixed switching frequency. The sliding mode controller presented good results in various conditions, and the MRAS observer was able to produce good estimates in a wide speed range, although very low speed operation is still unsolved. Future works involves testing the robustness of the implemented SMC with DTC+SVM strategy against parameters variations and comparing different estimation methods.

Acknowledgment

The authors are grateful to CNPq – Conselho Nacional de Desenvolvimento Científico e Tecnológico – and FAPESP – Fundação de Amparo à Pesquisa do Estado de São Paulo – for the financial support and to Texas Instruments for the DSP donation.

References

[1] I. Takahashi and T. Noguchi, "A new quick response and high efficiency control strategy of an induction motor," *Industry Applications, IEEE Transactions on*, vol. 22, pp. 820–827, 1986.

[2] M. Depenbrock, "Direct self-control (DSC) of inverter-fed induction machine," *Power Electronics, IEEE Transactions on*, vol. 3, no. 4, pp. 420–429, 1988.

[3] C. Lascu, I. Boldea, and F. Blaabjerg, "Direct torque control of sensorless induction motor drives: a sliding-mode approach," *Industry Applications, IEEE Transactions on*, vol. 40, no. 2, pp. 582–590, 2004.

[4] G. Buja and M. Kazmierkowski, "Direct torque control of PWM inverter-fed AC motors - a survey," *Industrial Electronics, IEEE Transactions on*, vol. 51, no. 4, pp. 744–757, 2004.

[5] J. Hung, W. Gao, and J. Hung, "Variable structure control: a survey," *Industrial Electronics, IEEE Transactions on*, vol. 40, no. 1, pp. 2–22, 1993.

[6] V. Utkin, J. Guldner, and J. Shi, *Sliding Mode Control in Electromechanical Systems*. CRC Press, 1999, iSBN: 0748401164.

[7] C. Schauder, "Adaptive speed identification for vector control of induction motors without rotational transducers," *Industry Applications, IEEE Transactions on*, vol. 28, no. 5, pp. 1054–1061, 1992.

[8] P. Jansen, R. Lorenz, and D. Novotny, "Observer-based direct field orientation: analysis and comparison of alternative methods," *Industry Applications, IEEE Transactions on*, vol. 30, no. 4, pp. 945–953, 1994.

[9] P. Vas, *Sensorless Vector and Direct Torque Control*. Oxford University Press, 1998, iSBN: 0198564651.

[10] M. P. Kazmierkowski, *Control in Power Electronics: Selected Problems (Academic Press Series in Engineering)*. Academic Press, 2002.

[11] Y. Xue, X. Xu, T. Habetler, and D. Divan, "A low cost stator flux oriented voltage source variable speed drive," in *Industry Applications Society Annual Meeting, 1990., Conference Record of the 1990 IEEE*, 1990, pp. 410–415 vol.1.